Zaria Journal of Electrical Engineering Technology, Department of Electrical Engineering, Ahmadu Bello University, Zaria – Nigeria. Vol. 9 No. 2 September, 2020. ISSN: 0261 – 1570.

ANALYTICAL ESTIMATION OF FLOW INDUCED VIBRATION IN PIN-PIN SUPPORTED PIPLELINE AND ITS ASSESSMENT AS BASE EXCITATION SIGNAL FOR A POWER HARVESTER

B. Usman
Department of Electrical Engineering, Bayero University, Kano, Nigeria

Keywords: –
Flow induced vibration, Pipeline, Pin-Pin Configuration, Power Harvesting, Piezo-electric generation, Fast Fourier Transform.

Article History: –
Received: July, 2020.
Reviewed: August, 2020
Accepted: September, 2020
Published: September, 2020

ABSTRACT

This work estimates analytically, the vibration induced in a simply supported pipeline with fluid flow, and assesses the vibration for its adequacy as base excitation signal for power harvesting transducer. The work is based on the model of the fourth order Partial and Ordinary Differential Equations without its Coriolis component. The Algorithms for the analytical solution of the FIV models are developed using the variable separation method, and lateral acceleration then simulated using MATLAB. The Fast Fourier Transforms of the obtained vibrations (acceleration) at different positions along the pipeline indicates that frequency and amplitude vary for different positions. For a set of adopted pipeline parameters and at a fluid flow velocity of 2 m/s, the maximum frequency is obtained at the centre of the pipe with amplitude of 10.64 m/s^2 at frequency of 41Hz. The values fall within the acceptable range of vibration that can be used for power harvesting applications.

1. INTRODUCTION

Energy has been essential in building up modern society. It is required everywhere and can be found from many different places in a different form. According to the Energy Theory, energy will never disappear, but they can be converted from one form to the other. Among many types of energy, electricity is the mostly needed for modern devices. Many researches are investigating methods of obtaining electrical energy from the ambient environment (AbdRahman 2011 , Huidong 2014, Zhang H 2015, Cao 2017) in the non-traditional ways, termed energy harvesting-Energy harvesting relates to the practice of scavenging small amounts of energy from ambient environmental sources such as wind, water, heat or vibrations in order to power either some small, low power electronic system directly, or to charge an electrical storage reservoir (usually a rechargeable battery or capacitor) that can be used to power a higher power application at time intervals.

Vibration energy is ubiquitous and potentially suitable for energy harvesting in numerous aspects of human experience, including natural events (seismic motion, wind, water tides) (Czerwinski 2014), common household goods (fridges, fans, washing machines, microwave ovens etc.), (Sojan 2016) industrial plant equipment, moving structures such as automobiles and aero planes, structures such as buildings, pipelines and bridges. Pipelines form one of the global structures, and the most efficient and cost-effective means of fluid transportation. They are mainly situated at remote or inaccessible area, where monitoring and surveillance of the pipe can be difficult. If sensors are use in such situations accessing the sensors to replace battery can be difficult. Therefore, harvesting energy from the environment can be one of the best options for continuous operation of the sensors.

A common existing model for the study of piezoelectric generators is the one based on the single-degree-of freedom (SDOF) modelling approach proposed by (Daqaq 2009) and (DuToit 2005), and is based on the configuration shown in Figure 1. This model requires two major inputs: the base excitation acceleration ($\ddot{x}_b$), and the tuned frequency of the piezoelectric generator model. It is common to use arbitrary sinusoidal signal without consideration for the broadband nature of a flow induced vibration (FIV).

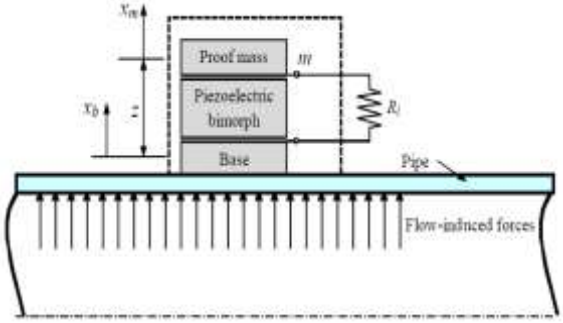

Figure 1: Configuration of a piezoelectric bimorph excited by a flow induced vibration in a pipeline

The study of flow induced vibration (FIV) in pipelines for power harvesting is not well looked into, the few current related works (Arafa 2010, Eziwarman, Forbes et al. 2012, Abd El-Mageed 2014) have not fully considered the sensitivity dependence of the pipeline on support and boundary conditions, such as simply supported, cantilever support, fixed ends supports and so on. As part of contributions to the literature in the understanding of the

effects of types of supports on the power harvesting from FIV in pipelines, this work will -study analytically, pipe flow induced vibrations in a simply supported pipeline span, and assess the resulting signals for power harvesting application. The study would consider flow induced vibration in a simply supported pipeline using available

2. MATERIALS AND METHODS

The major materials for this work are deflection model of a fluid conveying pipeline, and computing facilities and MATLAB software with statistical tools and Fourier analysis tools. The methods employed include the presentation and analytical solution of the deflection model and the simulation and generation of the excitation signals based on the analytical solutions (covered in this Section), and the analyses of the generated signals using statistical and Fourier analyses tools, the presentations and discussions of the observed trend from the simulations (covered in Section 3). These steps are represented in Figure 2.

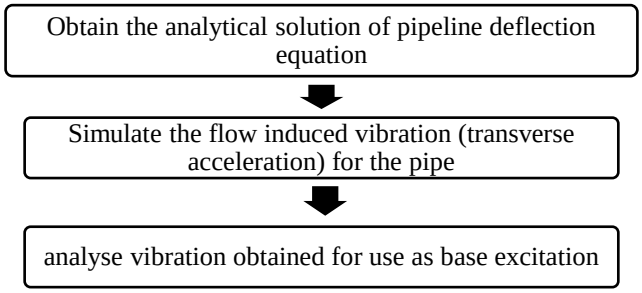

Figure 3: Computational algorithm of the output acceleration

Where the force components of Equation (1) are defined as follow:

$EI\frac{\partial^4 y}{\partial x^4}$ represents the elastic force experienced by material as it vibrates.

$\rho_f A v^2 \frac{\partial^2 y}{\partial x^2}$. represents the centrifugal force.

$2\rho A v \frac{\partial^2 y}{\partial x \partial t}$ is the *Coriolis* component which represents the force required to rotate the fluid element as

The deflection Equation (1) is both an initial value, and a boundary value problem. The Coriolis force in the equation does not dissipate energy or supply any energy in a conservative system (Chen 1985). Thus, by ignoring

model of flow induced vibration in a pipeline based on the Euler-Bernoulli beam theory, and then develops an analytical algorithm to obtain and quantify the vibration signal, principally its lateral acceleration. The simulations would be from first principle, using MATLAB. The generated signals from simulations will be analysed statistically and with Fast Fourier Transform (FFT) to assess its adequacy for base excitation applications in power harvesting.

In the following Section of this work, details of the materials and methods are presented, while in Section 3, the trends from the simulations are presented, followed by a discussion of the trends and the simulations in Section 4. The conclusions and recommendations resulting from the study are presented in Section 5.

3. DEFLECTION MODEL OF A PIPELINE CONVEYING FLUID

Consider a pipeline span segment shown in Figure 3, with homogeneous material properties and constant cross section that has a transverse deflection y from its equilibrium position. The length of the pipe is L, with internal pipe cross section A, modulus of elasticity E and area moment of inertia I. The pipe's mass per unit length is m_p and the density of the fluid flowing through it is ρ_f at a constant velocity v. The fluid is assumed to have a uniform velocity profile and incompressible.

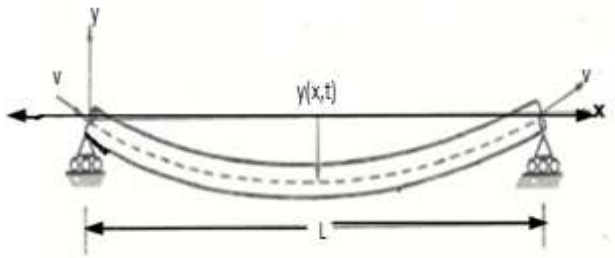

Figure 2: A fluid conveying pipeline with simple end supports

The governing equation for the transverse displacement y of the pipe with respect to time t and axial distance x is a nonlinear fourth order partial differential equation given by (Faal 2011, Avcar 2014)

$$EI\frac{\partial^4 y}{\partial x^4} + \rho_f A v^2 \frac{\partial^2 y}{\partial x^2} + 2\rho A v \frac{\partial^2 y}{\partial x \partial t} + \left(m_p + \rho_f A\right)\frac{\partial^2 y}{\partial t^2} = 0 \quad (1)$$

each point in the span rotates with an angular velocity.

$\left(m_p + \rho_f A\right)\frac{\partial^2 y}{\partial t^2}$ represents the inertial term or acceleration term.

the Coriolis term, the approximate governing equation for flow induced vibration in a pipeline approximates to:

$EI\frac{\partial^4 y}{\partial x^4} + (m_p + \rho_f A)\frac{\partial^2 y}{\partial t^2} + \rho_f A v^2 \frac{\partial^2 y}{\partial x^2} = 0$	(2)

Equation (2) may be solved analytically or numerically for the lateral deflection, y, lateral velocity $\dot{y}$, and lateral acceleration $\ddot{y}$, for all positions along the pipeline.

Analytical solution of the equation can be complex, especially since different configurations (different boundary and initial conditions) require different solutions. A simpler mass-spring-model description of the system requiring simpler solution is often adopted. Such simplifications can be found in the works of (Castillo 2001, Tiana 2016). However, this simple approach may not always provide solutions which are in very good agreement with real measurements. In this work, an analytical solution method is employed to study the lateral vibrations of the pipeline. The analytical solution of the deflection equation (2) is carried out using separation of variables method of solving partial differential equations and is presented in the following sub-Section.

4.ANALYTICAL SOLUTION OF THE DEFLECTION EQUATION

The particular solution of equation (2) depends on the boundary and initial conditions of the pipe. For freely supported (pin-pin) configuration, the boundary conditions (its deflection and bending moment at both ends of the pipe) and its initial conditions (initial deflections under its weight) are shown in Table 1.

Table 1: Boundary and initial conditions for pin-pin support

Boundary Conditions	Boundaries Deflection	$y\|_{(0,t)} = 0$	$y\|_{(L,t)} = 0$
	Boundaries Bending moment	$EI\frac{\partial^2 y}{\partial x^2}\Big\|_{(0,t)} = 0$	$EI\frac{\partial^2 y}{\partial x^2}\Big\|_{(L,t)} = 0$
Initial Conditions	Initial Deflection	$y\|_{(x,0)} = f(x) = \frac{wx}{24EI}(2Lx^2 - L^3 - x^3)$	
	Initial Velocity	$\frac{\partial y}{\partial t}\Big\|_{(x,0)} = 0$	

where w is weight per unit length of the pipeline.

Equation (2) can be written as:

$$\frac{\partial^4 y}{\partial x^4} + a\frac{\partial^2 y}{\partial t^2} + b\frac{\partial^2 y}{\partial x^2} = 0 \quad (3)$$

where

$$a = \rho_f A v^2/EI \qquad b = (m_p + \rho_f A)/EI$$

Using separation of variables method (Stroud 2003), a trial solution of Equation (3) may be written as:

$$y(x,t) = X(x)T(t) \quad (4)$$

$X(x)$ accounts for the lateral deflection with position only and $T(t)$ accounts for the lateral deflection with time only. Therefore, differentiating Equation (3) by parts and substituting in Equation (2) gives:

$$TX^{iv} + aTX'' + bX\ddot{T} = 0 \quad (5)$$

By variables separation, Equation (5) may be written as:

$$\frac{1}{T}(b\ddot{T}) = \frac{-1}{X}(X^{iv} + aX'') = \lambda \quad (6)$$

Equation (6) can be separated into two Ordinary Differential Equations (ODE) as:

$$b\ddot{T} - T\lambda = 0 \quad (7)$$

$$X^{iv} + aX'' + X\lambda = 0 \quad (8)$$

Since the problem is a vibratory one, physics requires that λ must be negative. Therefore, the characteristics equations for the ODEs above are given as:

$$bn^2 + \lambda = 0 \quad (9)$$

$$m^4 + am^2 - \lambda = 0 \quad (10)$$

Where $p^2 = m^4$

The roots of Equation (9) are:

$$n = \pm j\sqrt{\lambda/b} \quad (11)$$

The roots of Equation (10) are:

$$m_1 = \pm\sqrt{\left(\frac{-a + \sqrt{a^2 + 4\lambda}}{2}\right)}\ ;\ m_2 = \pm j\sqrt{\left(\frac{-a - \sqrt{a^2 + 4\lambda}}{2}\right)} \quad (12)$$

Therefore, the general solutions of the ODEs should be:

$$T(t) = A_1 cos(nt) + A_2 sin(nt) \quad (13)$$

$$\dot{T}(t) = -A_1 n sin(nt) + A_2 n cos(nt) \quad (14)$$

$$X(x) = B_1 cosh(m_1 x) + B_2 sinh(m_1 x) + B_3 cos(m_2 x) + B_4 sin(m_2 x) \quad (15)$$

$$X'(x) = B_1 m_1 sinh(m_1 x) + B_2 m_1 cosh(m_1 x) - B_3 m_2 sin(m_2 x) + B_4 m_2 cos(m_2 x) \quad (16)$$

$$X''(x) = B_1 m_1^2 cosh(m_1 x) + B_2 m_1^2 sinh(m_1 x) + B_3 m_2^2 cos(m_2 x) + B_4 m_2^2 sin(m_2 x) \quad (17)$$

Applying the boundary conditions for pin-pin support (From Table 1) at $X(0)$ gives:

$$B_1 = B_3 = 0 \quad (18)$$

Also, applying the boundary conditions $X(L) = 0$ gives:

$$B_2 = 0 \quad (19)$$

$$B_4 sinm_2 L = 0 \quad (20)$$

Non-trivial solution of Equation (20) requires that:

$$m_2 L = \pi, 2\pi, \dots, r\pi \quad r = 1, 2, 3, \dots \quad (21)$$

$$\Rightarrow m_2 = \alpha_r = \pi r/L$$

Therefore,

$$\lambda = \frac{1}{4}\left[\left(\frac{2\pi^2 r^2}{L^2} + a\right)^2 - a^2\right] = \frac{\pi^2 r^2}{L^2}\left(\frac{\pi^2 r^2}{L^2} + a\right) \quad (22)$$

And,

$$n = \omega_r = \sqrt{\frac{\lambda}{b}} = \sqrt{\frac{\pi^2 r^2}{bL^2}\left(\frac{\pi^2 r^2}{L^2} + a\right)} = \frac{\pi r}{L}\sqrt{\frac{1}{b}\left(\frac{\pi^2 r^2}{L^2} + a\right)} \quad (23)$$

Therefore, the general expression for the lateral deflection can be written as:

$$y(x,t) = B_4 sin\alpha_r x(A_1 cos\omega_r t + A_2 sin\omega_r t) \quad (24)$$

The expressions for α_r and ω_r for the first five modes are given in Table 1 below

Table 2: Eigenvalue expressions for some modes of pin-pin configuration

r	α_r	Eigenvalues (ω_r)		
		Rad/s	Hertz	Dimensionless
1	$\frac{\pi}{L}$	$\frac{\pi}{L}\sqrt{\frac{1}{b}\left(\frac{\pi^2}{L^2}+a\right)}$	$\frac{1}{2L}\sqrt{\frac{1}{b}\left(\frac{\pi^2}{L^2}+a\right)}$	$\pi L\sqrt{\left(\frac{\pi^2}{L^2}+a\right)}$
2	$\frac{2\pi}{L}$	$\frac{2\pi}{L}\sqrt{\frac{1}{b}\left(\frac{4\pi^2}{L^2}+\right.}$	$\frac{1}{L}\sqrt{\frac{1}{b}\left(\frac{4\pi^2}{L^2}+a\right.}$	$2\pi L\sqrt{\left(\frac{4\pi^2}{L^2}+\right.}$
3	$\frac{3\pi}{L}$	$\frac{3\pi}{L}\sqrt{\frac{1}{b}\left(\frac{9\pi^2}{L^2}+\right.}$	$\frac{3}{2L}\sqrt{\frac{1}{b}\left(\frac{9\pi^2}{L^2}+\right.}$	$3\pi L\sqrt{\left(\frac{9\pi^2}{L^2}+\right.}$
4	$\frac{4\pi}{L}$	$\frac{4\pi}{L}\sqrt{\frac{1}{b}\left(\frac{16\pi^2}{L^2}\right.}$	$\frac{2}{L}\sqrt{\frac{1}{b}\left(\frac{16\pi^2}{L^2}+\right.}$	$4\pi L\sqrt{\left(\frac{16\pi^2}{L^2}+\right.}$
5	$\frac{5\pi}{L}$	$\frac{5\pi}{L}\sqrt{\frac{1}{b}\left(\frac{25\pi^2}{L^2}\right.}$	$\frac{5}{2L}\sqrt{\frac{1}{b}\left(\frac{25\pi^2}{L^2}\right.}$	$5\pi L\sqrt{\left(\frac{25\pi^2}{L^2}\right.}$

The more general expression for the lateral deflection y and lateral velocity $\dot{y}$ are:

$$y(x,t) = \sum_{r=1}^{\infty} sin\alpha_r x(P_r cos\omega_r t + Q_r sin\omega_r t) \quad (25)$$

$$\dot{y}(x,t) = \sum_{r=1}^{\infty} \omega_r [sin\alpha_r x][-P_r sin\omega_r t + Q_r cos\omega_r t] \quad (26)$$

Applying initial conditions, of Table 1 give:

$$y|_{(x,0)} = f(x) = \sum_{r=1}^{\infty} P_r sin\alpha_r x \quad (27)$$

$$\dot{y}|_{(x,0)} = 0 = \sum_{r=1}^{\infty} \omega_r Q_r sin\alpha_r x \Longrightarrow Q_r = 0 \quad (28)$$

From Fourier series technique (Stroud & Booth, 2003), P_r is twice the mean of $\int_0^L f(x)\, sin\alpha_r x dx$, so we can write:

$$P_r = \frac{2}{L}\int_0^L f(x)\, sin\alpha_r x dx \quad (29)$$

Thus:

$$P_r\left(\frac{12(L)(EI)}{w}\right) = \int_0^L (2Lx^3 - L^3 x - x^4) sin\frac{r\pi}{L} x dx \quad (30)$$

Integration by parts give:

$$P_r\left(\frac{12(L)(EI)}{w}\right) = \left[\frac{(L^4 x - 2L^2 x^3 + Lx^4)}{r\pi} cos\frac{r\pi}{L}x + \frac{(6L^3 x^2 - L^5 - 4L^2 x^3)}{r^2\pi^2} sin\frac{r\pi}{L}x + \frac{(12L^4 x - 12L^3 x^2)}{r^3\pi^3} cos\frac{r\pi}{L}x + \frac{(24L^4 x - 12L^5)}{r^4\pi^4} sin\frac{r\pi}{L}x + \frac{24L^5}{r^5\pi^5} cos\frac{r\pi}{L}x\right]_0^L \quad (31)$$

Therefore,

$$P_r = \left(\frac{2wL^4}{\pi^5 EI}\right)\left(\frac{1}{r^5}\right)(cos\pi r - 1) \quad (32)$$

Therefore, the expressions for lateral deflection, lateral velocity and lateral acceleration are given respectively as:

$y(x,t) = \sum_{r=1}^{\infty} (P_r sin\alpha_r x)(cos\omega_r t)$	(33)
$\dot{y}(x,t) = -\sum_{r=1}^{\infty} (P_r \omega_r sin\alpha_r x)(sin\omega_r t)$	(34)
$\ddot{y}(x,t) = -\sum_{r=1}^{\infty} (P_r \omega_r^2 sin\alpha_r x)(cos\omega_r t)$	(35)

5. SIMULATION AND ANALYSIS OF THE PIPELINE FIV

The analytical solutions of the FIV model of a simply supported pipeline derived in Equations 33-35 are simulated in MATLAB. The simulation are performed based on a single pipeline span with the parameters specified in (Arafa 2010) and given in Table 3.

Table 3: Material properties of the pipe and fluid

FIV Properties	Faal R T & Derakshan D (2011)	Yunfeng et al (2020)	Arafa M et al (2010)
Density of pipe, ρ_p (kg/m^3)	7747	7850	8500
Density of fluid, ρ_f (kg/m^3)	997	999.8	1.225
Length of the pipe, L (m)	2	4	1.7
Modulus of elasticity, E (GPa)	207	200	100
Pipe outer diameter, D_0 (m)	0.054	0.3556	0.05
Pipe inner diameter, D_i (m)	0.05	0.3376	0.0488

The simulations are approached as a three-dimensional problem using matrix computations, where each calculated displacement, velocity or acceleration is linked to a combination of defined mode (r), position along the pipeline (x), and time (t). Therefore, the simulation specifies a spectrum of n modes, and divides the pipeline length into Nx segments ($Nx+1$ nodes), and the simulation time into Nt segments ($Nt+1$ nodes). The simulation proceeds by first calculating purely modal values ω_r and λ_r such that $\omega_r \in \mathbb{R}^{n\times 1}$ and $\lambda_r \in \mathbb{R}^{n\times 1}$. Using the calculated modal values vectors, the 2-D modal-position computation of amplitudes A_x, B_x and C_x are calculated such that $A_x \in \mathbb{R}^{n\times(Nx+1)}$, $B_x \in \mathbb{R}^{n\times(Nx+1)}$ and $C_x \in \mathbb{R}^{n\times(Nx+1)}$. These are followed by 2-D modal-time computations of $cos\omega_r t$ and $sin\omega_r t$ such that $cos\omega_r t \in \mathbb{R}^{(Nt+1)\times n}$ and $sin\omega_r t \in \mathbb{R}^{(Nt+1)\times n}$. Thereafter, the 3-D dimensional array of values of lateral displacements $y(x,t)$, lateral velocity $\dot{y}(x,t)$ and lateral acceleration $\ddot{y}(x,t)$. For each mode, the acceleration array has dimension $\ddot{y}(x,t) \in \mathbb{R}^{(Nt+1)\times(Nx+1)}$. So, the total acceleration for the spectrum is the summation of the acceleration for the individual modes. Finally, the trends from the simulations are plotted and statistical and Fast Fourier Transform (fft) performed to investigate the predicted vibrations for piezo-electric application

6. PRESENTATION OF TRENDS AND DISCUSSIONS

Note that from Equation (37) that $P_r = 0$ at $r = 2, 4, 6, \cdots$, the first, second, third and higher modes in a spectrum occur when $r = 1, 3, 5, \cdots$. Using the frequency equations of Table 2 and parameters of Table 3, the natural frequencies for $v = 0$ obtained from this study compared to those of Faal R T & Derakshan D (2011), Yunfeng L et al (2020) and Arafa et al. (2010) for the first five modes of a spectrum are given in Table 4.

Table 4: Comparing Results

	This Study			Faal R T & Derakshan D (2011)	
Mode	ω_r (Rad/s)	ω_r (Hertz)	ω_r (Dimensionless)	ω_r (Hertz)	ω_r (Dimensionless)
1	176	28	10		4.1992
2	705	112	39		11.577
3	1586	252	89		22.696
4	2819	449	158		37.519
5	4405	701	247		56.047
Mode	This Study			Yunfeng L et al (2020)	
1	269.5	41.3	9.9		9.8696
2	1038.0	165.2	39.5		39.4784
3	2335.4	371.7	88.8		88.8264
4	4151.8	660.8	157.9		157.9137
5	6487.2	1032.5	246.7		-
Mode	This Study			Arafa et al. (2010)	
1	204.3	32.5	9.9	74.3	
2	817.2	130.1	39.5	203.7	
3	1838.7	292.6	88.8	399.0	
4	3268.9	520.3	157.9	-	
5	5107.6	812.9	246.7	-	

The values of the natural frequencies from Yunfeng L. *et al* (2020) is in very good agreement with the present study. Also, the FIV parameters used in the simulation (steel with larger diameter and longer length) are closer to real situation of a pipe conveying fluid for piezo-electric application and the parameters would be used for the rest of this study. A fluid flow velocity of 2 m/s would also be adopted as it is much lower than the critical velocity for the adopted configuration.

Using the parameters of Yunfeng L. *et al* (2020), the 3-D acceleration plot in time series for the spectrum is shown in Figure 4. The figure shows that the lateral acceleration is symmetrical about the mid-point of the pipeline, and it ranges from 0 at the supports, to about $\pm 15\ m/s^2$ at the centre.

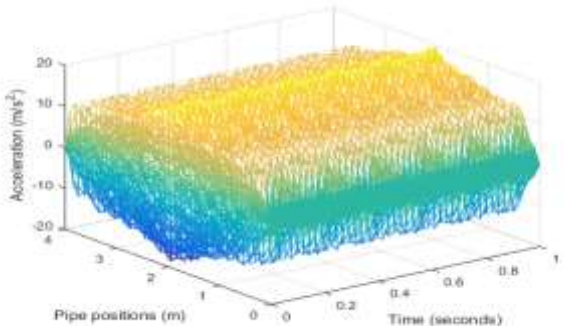

Figure 4: Lateral acceleration of the pipeline with respect to time and position along the pipeline

Two important information about the vibration environment are the acceleration amplitude and frequency. The acceleration determines the base excitation force (Basem 2015) (see Figure 2) while the frequency determines the tuning frequency of the piezo-electric generator. The trends of these two pieces of information are observed closely in this Section.

To see more closely the distribution of the acceleration along the pipe, it is divided into 12 equally spaced segments, or 13 points nodes along its length, as shown in Figure 5 (the number of segments is arbitrary, it could be more or less). The acceleration at the nodes is given in Figures 6 and 7 below.

Figure 5: Nodes along the pipeline

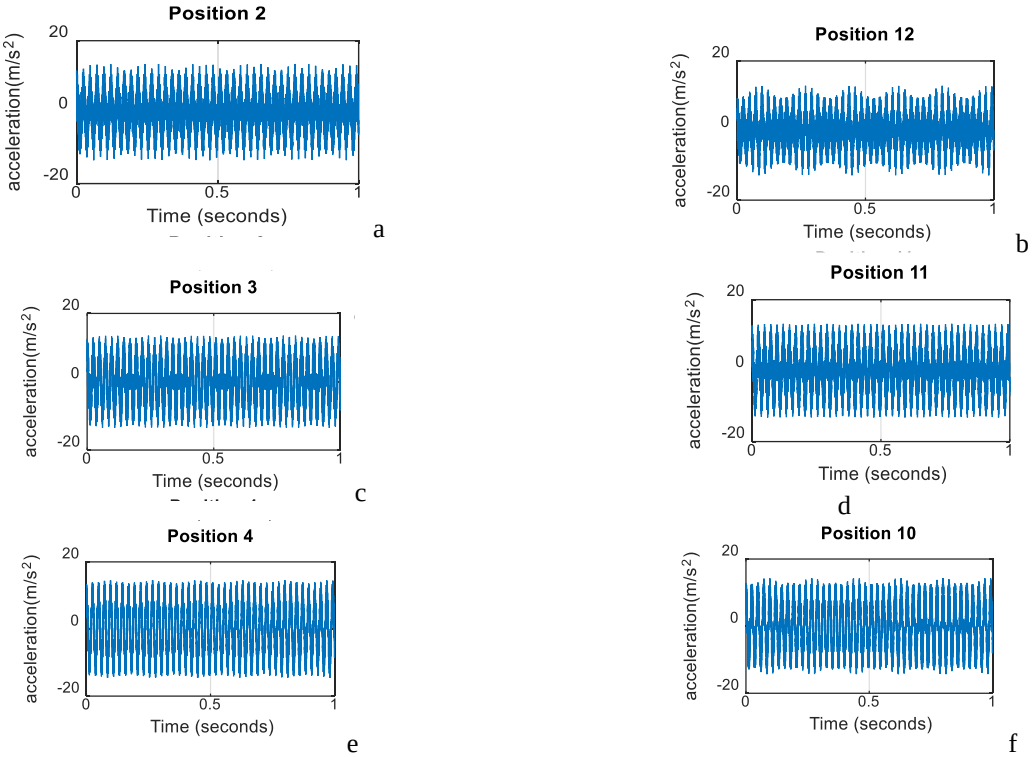

Figure 6: 2-D acceleration along the nodes of the pipeline (a – f)

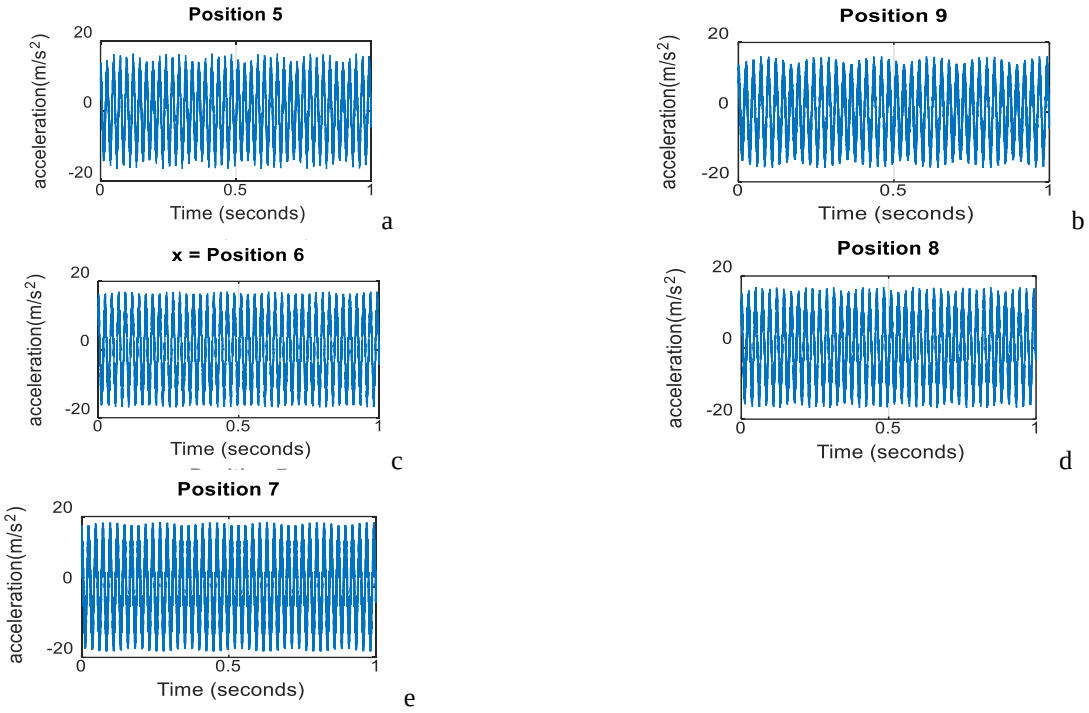

Figure 7: 2-D acceleration along the nodes of the pipeline (a – e)

The time series plots of Figures 6 and 7 show that the highest acceleration magnitudes occur at the centre of the pipeline (position 7 of Figure 7) and followed by nodes around the centre (position 6 and 8, 5 and 9 of Figure 7), and decrease towards the end of the pipeline (positions 4 and 10, 3 and 11 and 2 and 12 of Figure 6). The Figures show that for this configuration, excitation acceleration of up to 15 m/s^2 can be obtained at some locations along the pipe.

The time series of the two figures reveal only the magnitudes of the accelerations at these points and not more. To gain further insights, the Fast Fourier transforms (FFT) of the accelerations at these points are performed. To perform the FFT to cover the first five modes of the spectrum, we choose the sampling frequency to be at least 1200 Hz (at least twice the frequency of the last mode in the range of interest), in order to obtain a double-sided amplitude spectrum plots. With a chosen sampling frequency of 1200 Hz, values of frequency and associated amplitudes are presented in Table 5, while the single-sided amplitude spectrum plots of the FFT of the acceleration at the points are presented in Figures 8 and 9.

The plots show that the pipeline vibration frequency varies in amplitude at different positions along the pipe. In Figure 8, plots, positions 2 and 12, 3 and 11, and 4 and 10 are at symmetrical opposite points along the pipe respectively (see Figure 5). Likewise, in Figure 9, positions 5 and 9, 6 and 8 are at symmetrical opposite points along the pipe respectively. Position 7 is the mid-point. The figures show that piezo-electric generator tuned to a frequency of 41 Hz may be best located at the mid-point of the pipe, where the acceleration amplitude to up to 10.64, and the least desirable positions are those close to the end point, where acceleration amplitude is as low as 4.085. For higher frequency tuning of 371.7 Hz, locations towards the end points are better, where amplitude at this frequency is up to 4.082. Piezo-electric generator tuned to higher frequency than the above may be inappropriate for this configuration since amplitudes are very small at higher frequencies for all positions.

Table 5: Frequency and Amplitude at different positions along the pipeline

Frequency	Position along the pipeline and frequency amplitudes										
(Hz)	2	3	4	5	6	7	8	9	10	11	12
41	4.08	6.27	8.11	9.51	10.37	10.64	10.15	9.10	7.54	5.57	3.30
372	3.41	3.51	1.93	0.57	2.79	3.57	2.15	0.30	2.61	3.67	2.98
708	0.29	-	0.30	0.53	0.71	0.29	-	0.30	0.53	0.71	0.76
1033	1.70	-	1.69	1.30	0.71	1.70	-	1.69	1.30	0.71	1.84

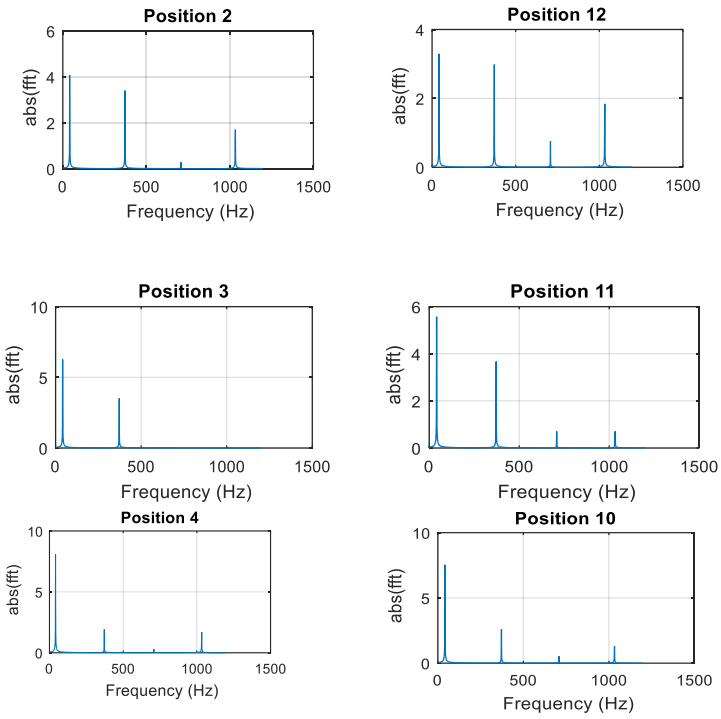

Figure 8: FFT plots along the nodes of the pipeline for positions 2, 3, 4, 10, 11 and 12

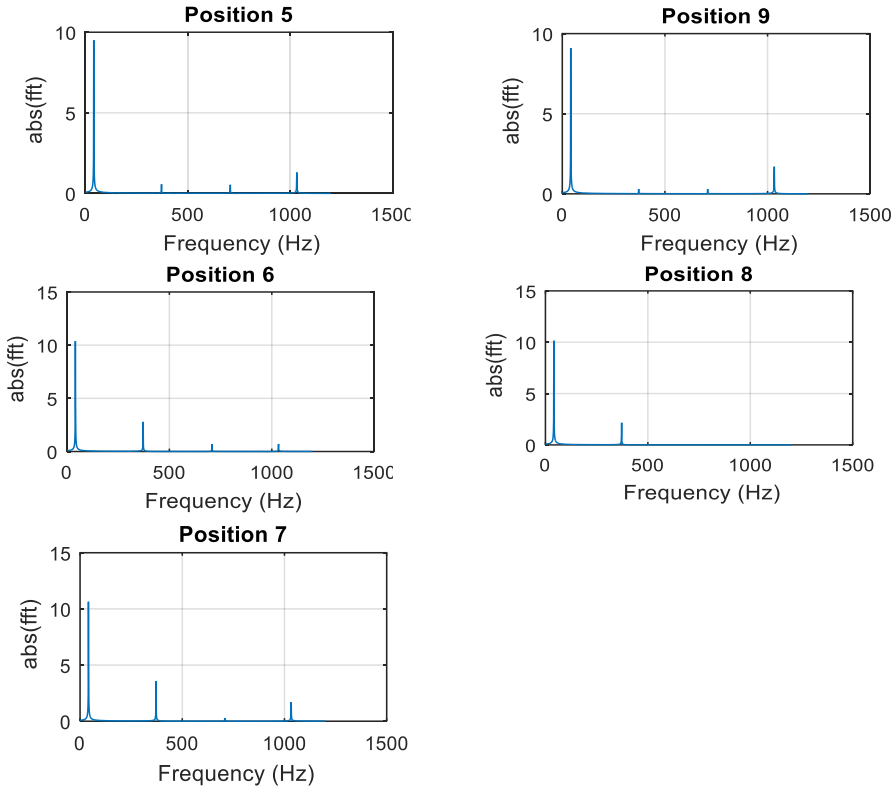

Figure 9: FFT plots along the nodes of the pipeline for positions 5, 6, 7, 8, and 9

Figure 10 is the combined FFT plot for the chosen configuration. The captured frequencies for the shown spectrum are 41, 372, 708 and 1033 Hertz. The plot shows that for any point, the best tuning frequency is 41 Hz, followed by 372 Hz.

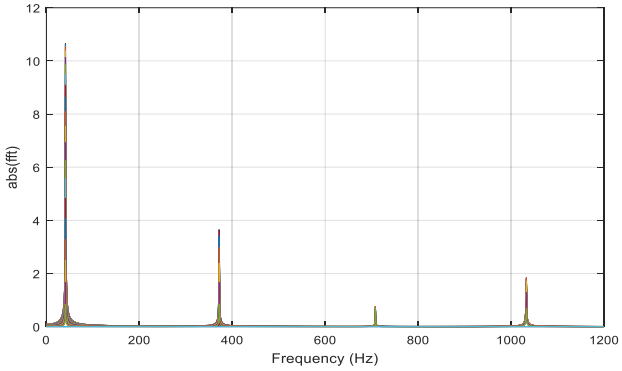

Figure 10: double sided amplitude spectrum of the pipeline vibration signal

The harvested power depends on the base excitation at the harvester location and therefore, the best position is at where an increase in pipe excitation is observed to offer an increased in harvested power. The highest power occurs when the pipe frequency matches the harvester frequency.

Most vibration data or signals used for vibration harvesting use harmonic signal (Marco Ferrari ; Vittorio Ferrari 2008), which is far from the common wide band vibration signal, but (Zero-Power 2015) proposes random signal and characterises the signal using exponential correlation noise which is a good approximation to real life vibration(Fox RF 1988). Therefore, the acceleration model in this work is also appraised using this procedure to ascertain its characteristics as compared to the real-world vibration signal. The plot is as shown in Figure 11, analysing the vibration data distribution shows it approximately resembles Gaussian distribution (Pittard 2004), similar to the distribution of signal used in the study of piezo-electric generators (Pittard 2004), (Zero-Power 2015) and (Shamim 2009).

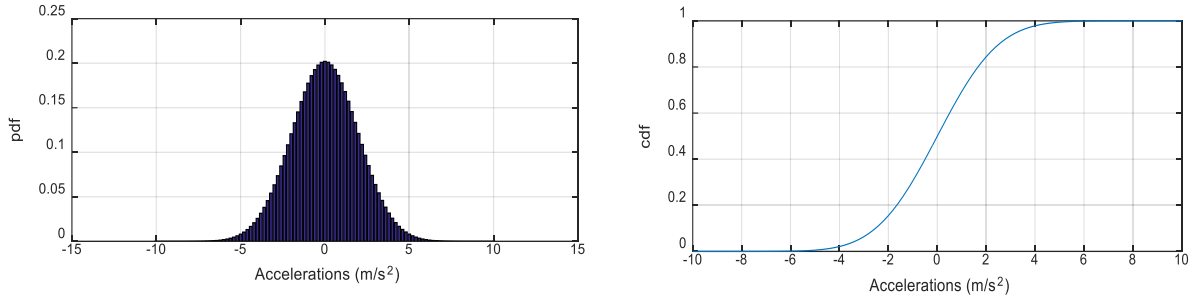

Figure 11: Distribution of the vibration along the pipe length

7. CONCLUSIONS

A first principle, analytical approach employing the variable separation method has been used to estimate the flow induced vibration of pipeline with pin-pin configuration based on an approximate beam theory of flow induced vibration in a pipeline. Using typical parameters of a fluid conveying pipeline, the pin-pin configuration is simulated for its lateral acceleration using MATLAB. The analytical solution shows that the pipeline natural frequency modes vary from 41 Hz, 165 Hz, 372 Hz, 660 Hz and 708Hz for Yunfeng L et al (2020) configuration. The simulated lateral acceleration trends are studied for suitability as excitation signals for piezo-electric applications using Fast-Fourier Transform (FFT) and statistical Probability Density Distribution (PDF). The FFT analyses shows that only tuning frequencies of 41 Hz, 372 Hz, and 708Hz are available for piezo-electric application, with the most one being 41 Hz, based on its high amplitude especially at the centre of the pipeline. The PDF analyses show that the distribution is gaussian, which has been shown in may publications to be suitable for piezo-electric applications.

REFERENCES

Abd El-Mageed, M. G., Arafa M, and Elaraby,M (2014). Simulation and Experimental Investigation of an Energy Harveater Utilizing Flow Induced Vibration. International Design Engineering Technical Conferences & Computers and Information in Engineering Conference DETC/CIE 2014 Buffalo, New York, USA.

AbdRahman, M. F. a. L. S. K. (2011). Investigation of Useful Ambient Vibration Sources for the Application of Energy Harvesting IEEE Student Conference on Research and Development Melaka, Malysia.

Arafa, M., Akl, W., Majeed, M., Al-Hussain, K. and Baz, A. (2010). Energy harvesting of gas pipeline vibration. Proc. of SPIE

Avcar, M. (2014). "Free Vibration Analysis of Beams Considering Different Geometric Characteristics and Boundary Conditions." International Journal of Mechanics and Applications **4**(3): 94-100.

Basem, M. B., Kerry, R. D. and Nikolai, D (2015). "Design Piezoelectric Energy Harvesting Using COMSOL for Mice Telemetry Device." Proceedings of the 2015 COMSOL Conference.

Cao, S. a. L., J (2017). "A survey on ambient energy sources and harvestingmethods for structural health

monitoring applications." Advances in Mechanical Engineering. **9**(4): 1-14.

Castillo, L. (2001). "Investigation of the Flow Induced Vibration in the E2 test Tacility." Rensselaer Polytechnic Institute, Troy, New York 12180, USA.

Chen, S. (1985). "FLOW-INDUCED VIBRATION OF CIRCULA CYLINDRICAL PIPES.".

Czerwinski, A., and Luczko, J. (2014). "Parametric Vibrations of Pipes Iinduced By Poulsating Flows in Hydraulic systems " Journal of theoretical and Applied Mechanics **52**(3): 719-730.

Daqaq, M. F., Inmana, D.J and Rennoa ,J.M (2009). "On the optimal energy harvesting from a vibration source." Journal of Sound and Vibration **320**: 386–405.

DuToit, N. E., Wardle, B. L., and Kim, S. (2005). "Design Considerations for MEMS-Scale Piezoelectric Mechanical Vibration Energy Harvesters, Integr. Ferroelectr." **71**: 121–160.

Eziwarman, G. L. Forbes and I. M. Howard (2012). Experimental Power Harvesting from a Pipe Using a Macro Fiber Composite (MFC). Proceedings of the 2011 2nd International Congress on Computer Applications and Computational Science: Volume 1. F. L. Gaol and Q. V. Nguyen. Berlin, Heidelberg, Springer Berlin Heidelberg**:** 443-449.

Faal, R. T., and Derakhshan, D (2011). Flow-Induced Vibration of Pipeline on Elastic Support. The Twelfth East Asia-Pacific Conference on Structural Engineering and Construction, Procedia Engineering

Fox RF, G. I., Roy R, Vemuri G. (1988). "Fast, accurate algorithm for numerical simulation of exponentially correlated colored noise." Phys Rev **38**(11): 5938-5940.

Huidong, L. C., T., and Daniel,D. Z. (2014). "Energy harvesting from low frequency applications using piezoelectric materials. ." Appl. Phys. Rev. .

Kreyszig, E. (2006). Advanced Engineering Mathematics. Singapore, John Wiley & Sons Inc

Marco Ferrari ; Vittorio Ferrari, M. G., Daniele Marioli, Andrea Taroni (2008). "Piezoelectric multifrequency energy converter for power Piezoelectric multifrequency energy converter for power harvesting in autonomous microsystems." Sensors and Actuators A 142 (2008) **A**(142): 329–335.

Nabeel K. Abid Al-Sahib , A. N. J., Osamah F. Abdulateef, (2010). "Investigation into the Vibration Characteristics and Stability of a Welded Pipe Conveying Fluid." Jordan Journal of Mechanical and Industrial Engineering **4** (3): Pages 378 - 387.

Pittard, M. T., Robert, P. E, Daniel, R. M, and Jonathan, D. B. (2004). "Experimental and numerical investigation of turbulent flow induced pipe vibration in fully developed flow." Review of Scientific Instruments **75**(7): 11.

Shamim, N. P. a. G. L. F. (2009). "Statistical Analysis of Vibration Modes of a Suspension Bridge Using Spatially Dense wireless Sensor Network." Journal of Structural Engineering.

Sojan, S., Kulkarni,R.K. (2016). "A Comprehensive Review of Energy Harvesting Techniques and its Potential Applications." International Journal of Computer Applications (0975 – 8887) **139**(No.3).

Stroud, K. A. (2003). Advanced Engineering Mathematics. New York, Palgrave Macmillan.

Tiana, J., Yuana, C., Yanga, L., Wua, C., Liua, G., and Yanga, Z. (2016). "The vibration analysis model of pipeline under the action of gas pressure pulsation coupling." Engineering Failure Analysis **66** 328–340.

Yunfeng Li1, Yundong Li, Naveed Akbar (2020), Analysis of Vibration of the Euler-Bernoulli Pipe Conveying Fluid by Dynamic Stiffness Method and Transfer Matrix, Journal of Applied Mathematics and Physics, Vol 8, pp 172-183

Zero-Power, C.-o. R. E. T. (2015). Benchmarking tools for vibration energy harvesting.

Zhang H, M. T. (2015). "Roles of the Excitation in Harvesting Energy from Vibrations." PLoS ONE **10** (10).